

2021

## Performance Enhancement in CZTS Solar Cells by SCAPS-1D Software

A. R. Latrous

*Higher Normal School "Assia Djebbar", Constantine, 25000, Algeria* \\ *LEA, Electronics Department, Batna2 University "Mostefa Ben Boulaid", Batna, 05000, Algeria, redha.latrous@gmail.com*

R. Mahamdi

*LEA, Electronics Department, Batna2 University "Mostefa Ben Boulaid", Batna, 05000, Algeria, redha.latrous@gmail.com*

B. N. Touafek

*LEA, Electronics Department, Batna2 University "Mostefa Ben Boulaid", Batna, 05000, Algeria* \\ *Higher National School of Biotechnologie "Toufik Khaznadar", Constantine, 25000, Algeria, redha.latrous@gmail.com*

M. Pasquinelli

*Detect Department, IM2NP Laboratory, UMR CNRS 7334, Aix-Marseille University, Marseille, 13000, France, redha.latrous@gmail.com*

Follow this and additional works at: <https://digitalcommons.aaru.edu.fo/ijtfst>

### Recommended Citation

R. Latrous, A.; Mahamdi, R.; N. Touafek, B.; and Pasquinelli, M. (2021) "Performance Enhancement in CZTS Solar Cells by SCAPS-1D Software," *International Journal of Thin Film Science and Technology*. Vol. 10 : Iss. 1 , Article 8.

Available at: <https://digitalcommons.aaru.edu.fo/ijtfst/vol10/iss1/8>

This Article is brought to you for free and open access by Arab Journals Platform. It has been accepted for inclusion in International Journal of Thin Film Science and Technology by an authorized editor. The journal is hosted on [Digital Commons](#), an Elsevier platform. For more information, please contact [rakan@aarj.edu.fo](mailto:rakan@aarj.edu.fo), [marah@aarj.edu.fo](mailto:marah@aarj.edu.fo), [u.murad@aarj.edu.fo](mailto:u.murad@aarj.edu.fo).

# Performance Enhancement in CZTS Solar Cells by SCAPS-1D Software

A. R. Latrous<sup>1,2,\*</sup>, R. Mahamdi<sup>2</sup>, B. N. Touafek<sup>2,3</sup> and M. Pasquinelli<sup>4</sup>

<sup>1</sup>Higher Normal School "Assia Djebar", Constantine, 25000, Algeria

<sup>2</sup>LEA, Electronics Department, Batna2 University "Mostefa Ben Boulaid", Batna, 05000, Algeria

<sup>3</sup>Higher National School of Biotechnologie "Toufik Khaznadar", Constantine, 25000, Algeria

<sup>4</sup>Detect Department, IM2NP Laboratory, UMR CNRS 7334, Aix-Marseille University, Marseille, 13000, France

Received: 21 Sep. 2020, Revised: 22 Nov. 2020, Accepted: 2 Dec. 2020.

Published online: 1 Jan. 2021

**Abstract:** This is the abstract, usually it does not have references. Usually the reader will read this part first to know what this paper is about and decide upon it to continue reading or not. The font of main text is 10 Times New Roman with single line spacing of 6 pt after and 0 pt before. The titles of sections are font 12, bold and they have single line spacing of 6pt before, 12 pt after, subsections are font 12, Italic and they have single line spacing of 6pt before, 12 pt after. Both upper line and lower line enclosing this part is paper-specific and changes according to the paper, usually it is very similar to the journal header background color, abstract contents are Times New Roman size 10, no line spacing.

**Keywords:** Absorber thin layer, Back metal contact, Efficiency, Solar cell.

## 1 Introduction

Nowadays, the industry of solar cells [1-5] is based more particularly on the production of the thin-film semiconductor Chalcopyrite Cu(In,Ga)Se<sub>2</sub> (CIGS) absorber layers, because of their high efficiency more than 20 % [6] compared to the others currently available, in addition to CdTe which also represents another absorber thin layer in terms of efficiency. However, considerable difficulties such as the excessive price, the scarcity of Indium (In) and the high toxicity of Cadmium (Cd) limit the use of CIGS and CdTe as absorber thin layers in cells solar technology. These constraints will constitute an obstacle for the further development of these types of solar cells in the near future, which has allowed researchers to develop new very reliable alternative absorber layers. That's why a great challenge has been lunched over the past decade regarding solar energy and in particular the thin-film Kesterite Cu<sub>2</sub>ZnSn(S,Se)<sub>4</sub> quaternary absorber materials given the abundance of their precursors (Zn, Sn), their low cost and especially their direct band gap (~ 1.5 eV), in addition to their high absorption coefficients (> 10<sup>4</sup> cm<sup>-1</sup>) [7,8], in replacement of their neighbors the CIGS whose structure is similar. Researchers such as Wei Wang et al were able to achieve an efficiency of around 12.6% using an

experimental protocol based on a pure hydrazine solution [9]. Thus, Kesterite have become more competitive and more promising with regard to photovoltaic energy conversion [10]. The pure CZTS solar cell possesses a low efficiency of 9% [11] was achieved in 2016, which is lower when compared with the theoretical efficiency. To reduce defects, impurities, and the secondary phases effects of the CZTS structure limiting the open circuit voltage (VOC) because of the losses caused by the different recombination mechanisms [12], and in order to increase the efficiency of the solar cell, we use a SCAPS 1-D simulation software (Solar Cell Capacitance Simulator) developed by the University of Gent which also allows to analyze the different families of solar structures, CIGS, CuInSe<sub>2</sub>, families of crystalline solar cells Si and GaAs as well as the families of amorphous a-Si cells [13,14]. The numerical modeling for heterojunctions with thin poly-crystalline films is very complex in reality, it is why, the use of this simulator having a large number of electrical measurements under darkness and under illumination and at different temperatures, allows to study variation effects of the different parameters of the solar cell on the output performance in order to calculate the open circuit voltage VOC, the short circuit current density JSC, the fill factor FF, and the quantum efficiency QE. The goal of our work is in a first phase to validate the proposed baseline structure with the experimental results, and in a second phase to

\*Corresponding author E-mail: [redha.latrous@gmail.com](mailto:redha.latrous@gmail.com)

improve its conversion efficiency by optimizing the absorber layer thickness, the acceptor carrier concentration of absorber layer and analyse the predominant effect of electron work function of the back metal contact. More details on the proposed structure and the numerical calculations will be exposed in the following sections.

## 2 Methodology and Device Structure

The model of the SCAPS-1D simulator is used to solve a number of one-dimensional equations systems for basic semiconductors, namely the Poisson and continuity equations for electrons and for holes, taking into account the conditions at the limits of interfaces and contacts [14]. This leads in a system of coupled differential equations in  $(\psi, n, p)$ . From our developed model, the graphical interface of the SCAPS software allowed to introduce four layers in (Fig.1), the molybdenum as back contact (Mo) followed by the MoS<sub>2</sub> layer with a band gap 1.7 eV for a thickness 0.1  $\mu\text{m}$ , the p-type absorber layer CZTS with a band gap 1.5 eV for variable thickness, the n-type buffer layer CdS with a band gap 2.4 eV for a thickness 0.05  $\mu\text{m}$ , and a front contact window layer ZnO:Al with a band gap 3.3eV for a thickness 0.2  $\mu\text{m}$ .

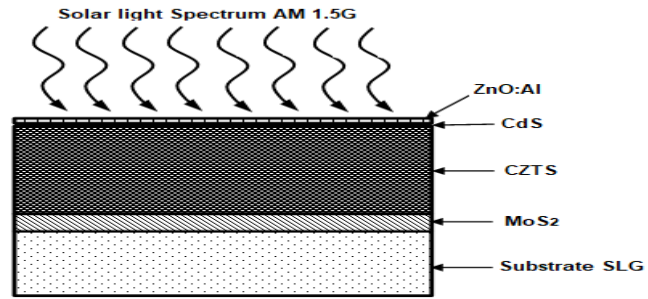


**Fig. 1:** Basic structure of the proposed CZTS solar cell.

Our cell thus modeled was exposed under a solar light spectrum AM 1.5G from its front contact for a power of 1 (kW/m<sup>2</sup>) and a temperature of 300° K. Under lighting, overabundance free carriers are created and the Fermi level divides into the quasi Fermi levels [15]. This detachment between the quasi-Fermi levels is responsible for the open circuit voltage VOC of the structure. Before starting the simulation, the internal reflection and transmission were adjusted at the front contact. In this simulation, defects of the different layers are taken into account. For the absorber layer, they are considered to be donor type, while for the buffer layer, they are considered to be acceptor type.

**Table 1:** Simulation parameters for the device.

Cell properties	
Cell temperature T° [K]	300
series Resistance Rs [ $\Omega \cdot \text{cm}^2$ ]	4.25
Shunt Resistance Rsh [ $\Omega \cdot \text{cm}^2$ ]	400
Back metal contact properties	
Metal work function [eV]	Var
SRV* of electron [cm/s]	$10^5$
SRV* of hole [cm/s]	$10^7$
Front metal contact properties	
Metal work function	Flat band
SRV* of electron [cm/s]	$10^7$
SRV* of hole [cm/s]	$10^5$

**Table 2:** Physical parameters for the different layers

Parameters	MoS2	CZTS	CdS	ZnO:Al
Thickness [ $\mu\text{m}$ ]	0.1	Var	0.05	0.2
Bandgap $E_g$ [eV]	1.7	1.5	2.4	3.3
Electron affinity $\chi$ [eV]	4.2	4.5	4.5	4.6
Relative dielectric permittivity $\epsilon_r$ [eV]	13.6	10	10	9
Conduction band effective density of states $N_C$ [ $\text{cm}^{-3}$ ]	$2.2 \times 10^{18}$	$2.2 \times 10^{18}$	$2.8 \times 10^{19}$	$2.2 \times 10^{18}$
Valence band effective density of states $N_V$ [ $\text{cm}^{-3}$ ]	$1.8 \times 10^{19}$	$1.8 \times 10^{19}$	$2.4 \times 10^{18}$	$1.8 \times 10^{19}$
Electron thermal velocity [ $\text{cm/s}$ ]	$1 \times 10^7$	$1 \times 10^7$	$1 \times 10^7$	$1 \times 10^7$
Hole thermal velocity [ $\text{cm/s}$ ]	$1 \times 10^7$	$1 \times 10^7$	$1 \times 10^7$	$1 \times 10^7$
Electron mobility $\mu_n$ [ $\text{cm}^2/\text{V}\cdot\text{s}$ ]	$1 \times 10^2$	$1 \times 10^2$	$3.5 \times 10^2$	$1 \times 10^2$
Hole mobility $\mu_p$ [ $\text{cm}^2/\text{V}\cdot\text{s}$ ]	$2.5 \times 10^1$	$2.5 \times 10^1$	$5 \times 10^1$	$2.5 \times 10^1$
Donor density $N_D$ [ $\text{cm}^{-3}$ ]	$1 \times 10^1$	$1 \times 10^1$	$1 \times 10^{17}$	$1 \times 10^{18}$
Acceptor density $N_A$ [ $\text{cm}^{-3}$ ]	$1 \times 10^{16}$	Var	$1 \times 10^1$	$1 \times 10^5$
Absorption coefficient $\alpha$ [ $\text{cm}^{-1}$ ]	Scaps	Scaps	Scaps	Scaps
Radiative recombination coefficient $B_r$ [ $\text{cm}^3/\text{s}$ ]		$5 \times 10^{-9}$		
Auger electron capture coefficient [ $\text{cm}^6/\text{s}$ ]		$1 \times 10^{-29}$		
Auger hole capture coefficient [ $\text{cm}^6/\text{s}$ ]		$1 \times 10^{-29}$		
Defect density [ $\text{cm}^{-3}$ ]	-	D : $1 \times 10^{13}$	A : $6 \times 10^{16}$	-

Interface defects between absorber/buffer and buffer/window are neglected. The device and material parameters used in this study which were selected based on the experimental, literature values, theory, or from reasonable estimates are listed in Table 1 and Table 2 [15,16]. The front metal contact is considered as a standard flat band one while the back metal contact whose variable electron work function will allow to optimize the output performance of the considered structure. The effects of radiative recombination and Auger electron/hole captures were introduced in the simulation. In addition, absorption coefficient values  $\alpha$  for all the layers of the structure are considered to be variable in the calculations.

### 3 Results and Discussions

#### 3.1 The Basic CZTS Simulation and Validation

In order to validate the proposed baseline MoS<sub>2</sub>/p-CZTS/n-CdS/ZnO:Al structure before optimization, we have drawn the energy bands by highlighting the offset of the conduction and valence bands. When the hetero-junction formed, the Fermi level of all layers aligns and all the bands line up accordingly at equilibrium along with the vacuum level. Energy band discontinuity is the major concern for the heterojunction based thin film photovoltaic devices. A Schottky contact is formed at CZTS/MoS<sub>2</sub> interface from the fact that the work function of Mo (5 eV) is less than that

of CZTS (~6.0 eV). The graphical energy band diagrams of the structure for the non-equilibrium condition are shown in (Fig.2).

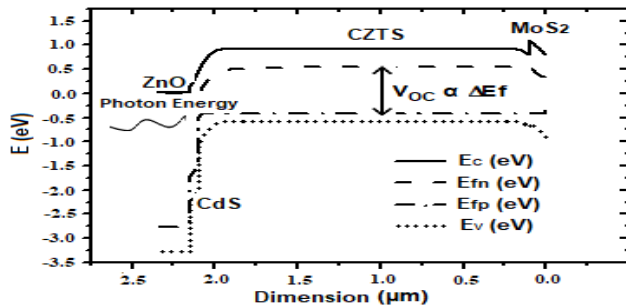


**Fig. 2:** Energy band diagram of the CZTS structure under illumination before optimization.

The superposition of the simulated characteristic J-V of the proposed structure obtained with the data of Table 1 and Table 2, before optimization with that of the experimental in (Fig.3) shows a good agreement. The values obtained exhibit an efficiency of 6.77 % for an absorber layer thickness of 3.0  $\mu\text{m}$ , a concentration of acceptor atoms of  $3 \times 10^{16} \text{ cm}^{-3}$ , with a good compromise with reported experimental results using similar structure generated by sputtering and vacuum evaporation techniques, respectively [17]. This will allow us throughout our work to optimize the parameters of the proposed structure and improve its performance. So, we will study the effects of absorber layer thickness, acceptor carrier concentration and the electron work function of the back metal contact by fixing the parameters values of the other layers (ZnO:Al, CdS and MoS2).

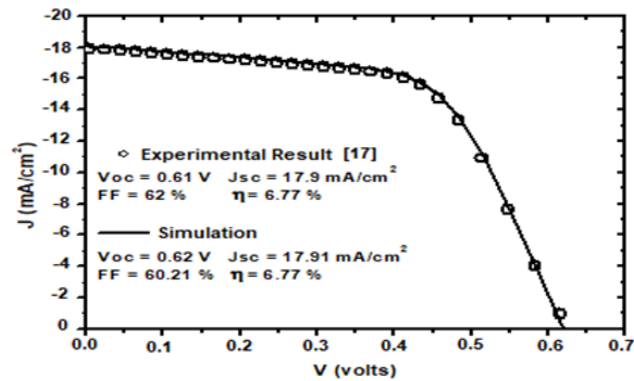


**Fig. 3:** Comparison between simulated and experimental J-V characteristics of the CZTS structure before optimization.

### 3.2 Effect of Absorber Layer Thickness

The thickness of the absorber layer is the most important parameter [18-21]; it constitutes almost the entire dimension of the thin-film solar structure. It represents the active layer of which the majority of photons having an energy greater than or equal to its band gap are absorbed, such as most of the photo generation and recombination mechanisms of the free carriers take place, however the length of carrier diffusion represents a constraint. One of the difficulties of the solar structure technology is to control the absorber layer thickness to obtain the best performance. The goal in this work is to vary the absorber layer thickness from 0.5  $\mu\text{m}$  to 5  $\mu\text{m}$ . In (Fig.4), we can observe its impact on the output parameters VOC, JSC, FF, and the efficiency.

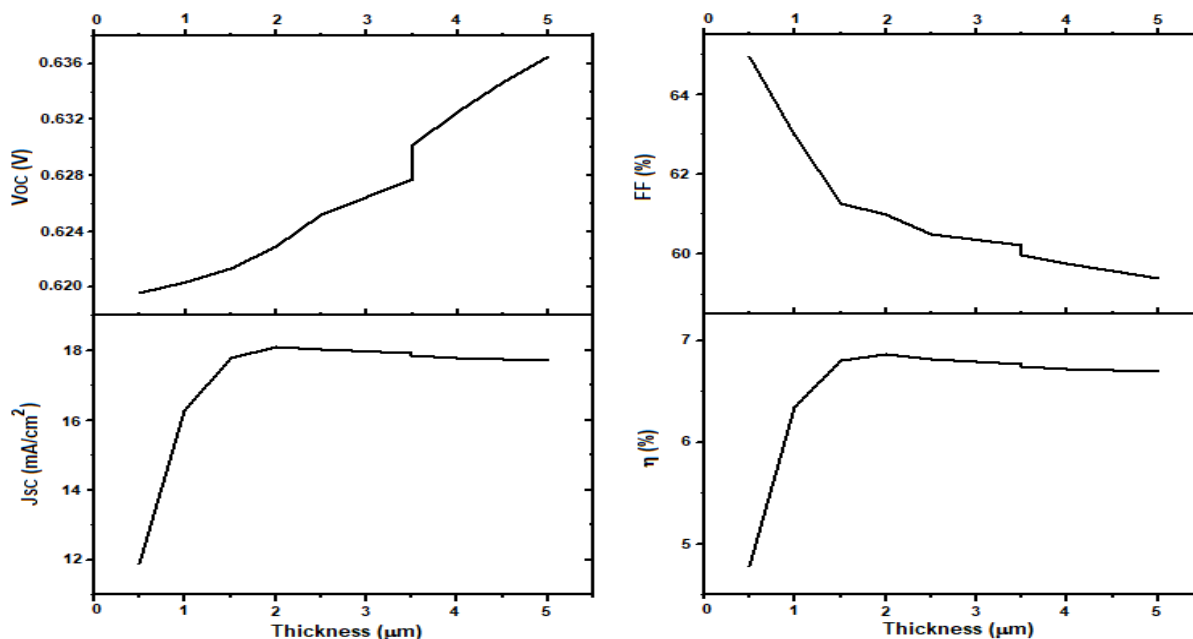


**Fig. 4:** Simulated output parameters as a function of absorber layer thickness of the CZTS structure.

JSC and VOC increase proportionally with the absorber layer thickness, and therefore the conversion efficiency of the entire proposed structure increases in turn. The short circuit current density JSC is ameliorated when the absorber thickness value exceeds 1.5 μm with an efficiency which follows the same shape and which saturates around 2 μm, while the fill factor FF decreases with thickness. In conclusion, the optimal value of the absorber thickness obtained for the best possible performance is 2 μm.

### 3.3. Effect of Acceptor Carrier Concentration of Absorber Layer

The acceptor carrier concentration NA is an important parameter whose influence on the performance of our proposed structure is simulated in this work. (Fig. 5) shows the variation of the output parameters VOC, JSC, FF and efficiency as a function of NA in the range 10<sup>15</sup> to 10<sup>18</sup> cm<sup>-3</sup>. It has been found that VOC increases with carrier concentration, while JSC decreases; this is explained by the existence of an electric field within the space charge region closely proportional to VOC. The mathematical model of the PN junction diode suitably illustrates this phenomenon [21].

$$I_0 = Aqn^2 \left( \frac{D_e}{L_e NA} + \frac{D_h}{L_h ND} \right). \quad (1)$$

$$V_{OC} = \frac{kT}{q} \ln \left( \frac{I_L}{I_0} + 1 \right). \quad (2)$$

The computed results are in good agreement with theory [15]. It has also been found that as NA increases, the conversion efficiency degrades, and therefore the control of this parameter is one of the most relevant preoccupation of research [22,23]. The optimized parameter of the acceptor carrier concentration is calculated for the value of 1×10<sup>16</sup> cm<sup>-3</sup>, which makes it possible to acquire the best performance for the structure.

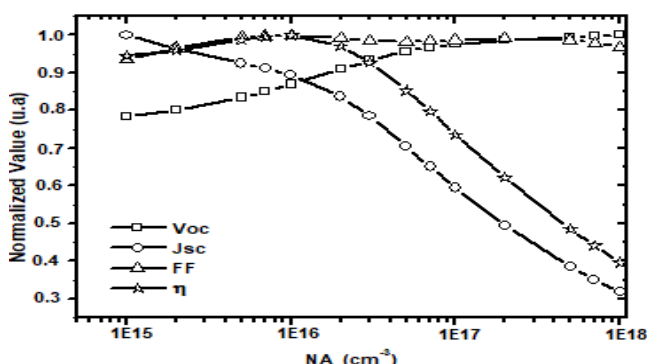


Fig. 5: Normalized output parameters (VOC, JSC, FF, η) as a function of acceptor carrier concentration of the CZTS structure.

### 3.4 Effect of the Back Metal Contact

Another parameter of great technological importance for solar structures is the back metal contact [24-26]. In (Fig. 6), the value of electron work function has been varied in the range of 5 to 6 eV to study its impact on the output performance of the proposed cell. At first it was observed that open circuit voltage and efficiency increased almost linearly with the metal work function for the same range from 5.0 to 5.5 eV. Thereafter, these two output quantities have kept an almost constant shape for the range of 5.5 eV to 6.0 eV. According to the simulation results, we can admit that the Platinum whose electron work function value is 5.7 eV represents the most suitable material that can replace the Molybdenum as back metal contact.

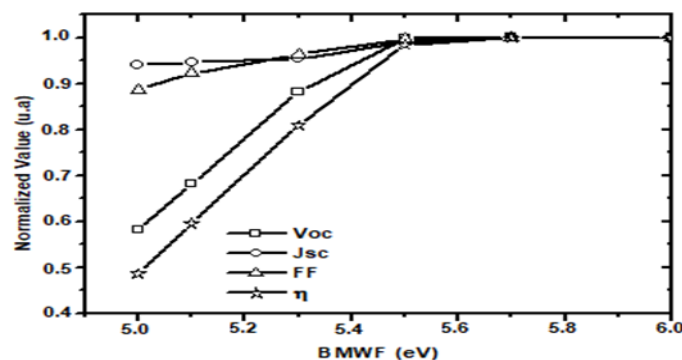


Fig. 6: Normalized output parameters (VOC, JSC, FF, η) as a function of electron work functions of back metal contact of the CZTS structure.

### 4 Optimization of the Proposed Structure

The J-V Characteristic of the proposed structure after optimization is shown in (Fig. 7). The optimized solar cell exhibits a much better performance for an efficiency of 15.23 % with JSC ≈ 21.9 mA/cm<sup>2</sup>, VOC ≈ 1 V, and FF = 69.79 %. By considering the simulation results, the output performances for the structure are computed for thickness of 2 μm, acceptor carrier concentration of 1×10<sup>16</sup> cm<sup>-3</sup> and electron work function of the back metal contact of 5.7 eV.

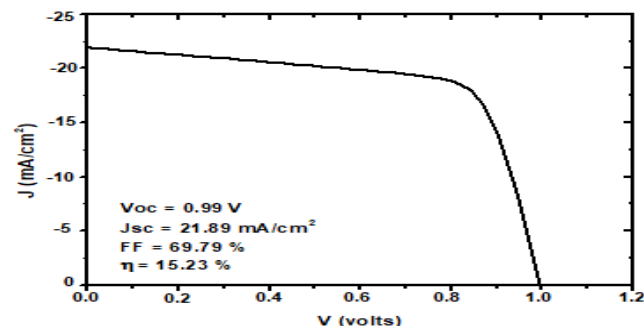
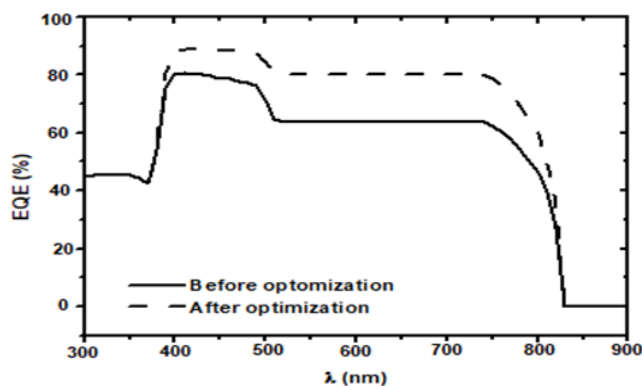


Fig. 7: Simulated J-V characteristic of the CZTS structure after optimization .

Calculated external quantum efficiency (EQE) for the entire structure before and after optimization is shown in (Fig. 8). On the graph, it has been observed a marked enhancement in the efficiency in the visible region.



**Fig. 8:** Comparison of the external quantum efficiency of the CZTS structure before and after optimization .

## 5 Conclusions

In a first phase of this paper, the proposed baseline MoS<sub>2</sub>/CZTS/CdS/ZnO:Al structure was simulated by the SCAPS-1D software, compared and validated with the experimental results. A good compromise of the conversion efficiency of 6.77% was found before optimization by using Molybdenum as back metal contact. In a second phase, to improve the performance of the solar structure, three parameters of the CZTS active layer were optimized; the absorber layer thickness, the acceptor carrier concentration and electron work function of the back metal contact. The optimized values of these parameters are 2.0 μm, 1×10<sup>16</sup> cm<sup>-3</sup> and 5.7 eV respectively. After optimization, JSC has increased by 3.98 mA/cm<sup>2</sup>, VOC has increased by 0.37 V and FF has increased by 7.79 % for an overall efficiency of 15.23 %. The numerical calculations have shown that Platinum as back metal contact and as a replacement for Molybdenum increases efficiency of the structure. Throughout this simulation, interface defects were neglected. So, an extension to this work consists in introducing them into the calculations to study their effects on the output performances of the structure.

## Acknowledgements

The authors would like to thank Dr. M. Burgelman from University of Gent for using SCAPS-1D program in all simulations reported in this paper.

## References

[1] A.K. Hussein, Applications of nanotechnology in renewable energies-A comprehensive overview and understanding, *Renewable and Sustainable Energy Reviews.*, **42**, 460-476(2015).

- [2] A.K. Hussein, A. Walunj, L. Kolsi, Applications of nanotechnology to enhance the performance of the direct absorption solar collectors, *Journal of Thermal Engineering.*, **2**, 529-540(2016).
- [3] D. Li, Z. Li, Y. Zheng, C. Liu, A.K Hussein, X. Liu, Thermal performance of a PCM-filled double-glazing unit with different thermophysical parameters of PCM, *Solar Energy.*, **133**, 207-220(2016).
- [4] A.K. Hussein, Applications of nanotechnology to improve the performance of solar collectors – Recent advances and overview, *Renewable and Sustainable Energy Reviews.*, **62** 767-792(2016).
- [5] A.K. Hussein, D. Li, L. Kolsi, S. Kata, B. Sahoo, A review of nano fluid role to improve the performance of the heat pipe solar collectors, *Energy Procedia.*, **109**, 417- 424(2017).
- [6] M.A Green, Y. Hishikawa, E.D. Dunlop, D.H. Levi, J. Hohl-Ebinger, A.W.Y. Ho-Baillie, Solar cell efficiency tables (version 52), *Prog. Photovolt. Res. Appl.*, **26**, 427-436(2018).
- [7] K. Jimbo, R. Kimura, T. Kamimura, S. Yamada, W.S. Maw, H. Araki, K. Oishi, H. Katagiri, Cu<sub>2</sub>ZnSnS<sub>4</sub>-type thin film solar cells using abundant material, *Thin Solid Films.*, **515**, 5997-5999 (2007).
- [8] H. Katagiri, K. Saitoh, T. Washio, H. Shinohara, T. Kurumadani, S. Miyajima, Development of thin film solar cell based on Cu<sub>2</sub>ZnSnS<sub>4</sub> thin film, *Solar Energy Materials and Solar Cells.*, **65**, 141-148(2001).
- [9] W. Wang, M.T. Winkler, O. Gunawan, T. Gokmen, T.K. Todorov, Y. Zhu, D.B. Mitzi, Device characteristics of CZTSSe thin film solar cells with 12.6% efficiency, *Adv. Energy. Mater.*, **4**, 1301465(2014).
- [10] M.S. Kumar, S.P. Madhusudanan, S.K. Batabyal, Substitution of Zn in Earth-Abundant Cu<sub>2</sub>ZnSn(S,Se)<sub>4</sub>-based thinfilm solarcells—A status review, *Solar Energy Materials and Solar Cells.*, **185**, 287-299(2018).
- [11] K. Sun, C. Yan, F. Liu, J. Huang, F. Zhou, J.A. Stride, M. Green, X. Hao, Over 9% Efficient Kesterite Cu<sub>2</sub>ZnSnS<sub>4</sub> Solar Cell Fabricated by Using Zn<sub>1-x</sub>Cd<sub>x</sub>S Buffer Layer, *Adv. Energ. Mater.*, **6** 1600046(2016).
- [12] S. Chen, J.H. Yang, X.G. Gong, A. Walsh, S.H. Wei, Intrinsic point defects and complexes in quaternary kesterite semiconductor Cu<sub>2</sub>ZnSnS<sub>4</sub>, *Physical Review B.*, **81**, 245204(2010).
- [13] M. Burgelman, J. Verschraegen, S. Degraeve, P. Nollet, Modeling thin-film devices, *Prog. Photovolt : Res.Appl.*, **11**, 1-11(2003).
- Information on <http://www.scaps.elis.ugent.be>.
- [14] M. Patel, A. Ray, Enhancement of output performance of Cu<sub>2</sub>ZnSnS<sub>4</sub> thin film solar cells—A numerical simulation approach and comparison to experiments, *Physica. B.*, **40**, 4391-4397(2012).
- [15] F.A. Jhuma, M.Z. Shaily, M.J. Rashid, Towards high-efficiency CZTS solar cell through buffer layer optimization, *Mat. Ren. Sust. Energy.*, **8**, 1-6(2019).
- [16] D.B. Mitzi, O. Gunawan, T.K. Todorov, K. Wang, S. Guha, The path towards a high performance solution-processed kesterite solar cell, *Sol. En. Mat.*, **95**, 1421-1436(2011).
- [17] S. Yaşar, S. Kahraman, S. Cetinkaya, S. Apaydın, I. Bilican, I. Uluer, Numerical thickness optimization study of CIGS based solar cells with wxAMPS, *Optik.*, **127**, 8827-8835(2016).
- [18] M.D. Wanda, S. Ouédraogo, F. Tchhoffo, F. Zougmore, J.M.B. Ndjaka, Numerical investigations and analysis of Cu<sub>2</sub>ZnSnS<sub>4</sub> based solar cells by SCAPS-1D, *Int. J. Photoenergy.*, **2016**, 1-9(2016).
- [19] A. Cherouana, R. Labbani, Study of CZTS and CZTSSe solar cells for buffer layer selection, *Appl. Surf.*, **424**, 251-255(2015).

- [20] J.H.N. Tchognia, Y. Arba, K. Dakhsi, B. Hartiti, A. Ridah, J.M. Ndjaka, P. Thevenin, Optimization of the output parameters in kesterite-based solar cells by AMPS-1D, Proceeding of the 3rd International Renewable and Sustainable Energy Conference (IRSEC), (2015).
- [21] C. Maykel, E. Valencia-Resendiz, F.A. Pulgarín-Agudelo, O. Vigil-Galán, Determination of minority carrier diffusion length of sprayed-Cu<sub>2</sub>ZnSnS<sub>4</sub> thin films, Solid State Electron., **118**, 1-3 (2016).
- [22] B. Liu, J. Guo, R. Hao, L. Wang, K. Gu, S. Sun, A. Aierken, Effect of Na doping on the performance and the band alignment of CZTS/CdS thin film solar cell, Solar Energy., **201** 219–226 (2020).
- [23] N.B. Michaelson, The work function of the elements and its periodicity, J. Appl. Phys., **48**, 4729-4733(1977).
- [24] F.Z. Boutebakh, M. Lamri Zeggar, N. Attaf, M.S. Aida, Electrical properties and back contact study of CZTS/ZnS heterojunction, Optik., **144**, 180-190(2017).
- [25] J.J. Scragg, J.T. Wätjen, M. Edoff, T. Ericson, T. Kubart, C. Platzer-Björkman, A Detrimental Reaction at the Molybdenum Back Contact in Cu<sub>2</sub>ZnSn(S,Se)<sub>4</sub> Thin-Film Solar Cells, J. Am. Chem. Soc., **134**, 19330–19333(2012).